PTEP

Prog. Theor. Exp. Phys. **2019**, 063B03 (26 pages)
DOI: 10.1093/ptep/ptz053

Numerical analyses of $\mathcal{N} = 2$ supersymmetric quantum mechanics with a cyclic Leibniz rule on a lattice

Daisuke Kadoh[1,2,*], Takeru Kamei[3,*], and Hiroto So[4,*]

[1]*Department of Physics, Faculty of Science, Chulalongkorn University, Bangkok 10330, Thailand*
[2]*Research and Educational Center for Natural Sciences, Keio University, Yokohama 223-8521, Japan*
[3]*Graduate School of Science and Engineering, Ehime University, Matsuyama 790-8577, Japan*
[4]*Physics Department, Ehime University, Matsuyama 790-8577, Japan*
[*]E-mail: kadoh@keio.jp, kamei.ehime@gmail.com, hiroto.so@gmail.com

Received April 22, 2019; Accepted April 25, 2019; Published June 23, 2019

We study a cyclic Leibniz rule, which provides a systematic approach to lattice supersymmetry, using a numerical method with a transfer matrix. The computation is carried out in $\mathcal{N} = 2$ supersymmetric quantum mechanics with the ϕ^6 interaction for weak and strong couplings. The computed energy spectra and supersymmetric Ward–Takahashi identities are compared to those obtained from another lattice action. We find that a model with the cyclic Leibniz rule behaves similarly to the continuum theory compared to the other lattice action.

Subject Index B15, B16, B38

1. Introduction

The difficulty in lattice supersymmetry (SUSY) originates from the lack of the Leibniz rule [1]. Since any local lattice difference operator does not obey the Leibniz rule [2,3], it is difficult to realize the full SUSY within a local lattice theory [1,4–6]. Several approaches in which part of SUSY is kept on the lattice and the full symmetry is restored at the continuum limit have been proposed so far [7–20]. Those are, however, the same in a sense that, without getting into details about the algebraic structure of a lattice Leibniz rule, nilpotent SUSY is realized on the lattice in various ways. The deep understanding of the lattice Leibniz rule could help us to define a lattice model naturally keeping as many symmetries as possible and to study higher-dimensional SUSY theories without fine tunings, or with fewer fine tunings.

In Ref. [21], another type of lattice Leibniz rule was proposed in $\mathcal{N} = 2$ SUSY quantum mechanics (QM) [22,23], which keeps some symmetries exactly. The indices of the new rule appear cyclically[1] and we refer to it as a cyclic Leibniz rule (CLR) in this paper, as did the authors of Ref. [21]. The CLR has many solutions and the general solution for a symmetric difference operator has been studied in Ref. [24]. $\mathcal{N} = 4$ SUSY QM and the $\mathcal{N} = 2$ SYK model are also defined on the lattice such that the half SUSY is exactly kept [25,26]. For those models, the exact invariance of half symmetry naturally leads to the CLR although there is another lattice formulation with an exact symmetry in $\mathcal{N} = 2$ SUSY QM [8]. Furthermore, a kind of non-renormalization theorem holds for the CLR action of the

[1] The difference between the standard Leibniz rule and the cyclic Leibniz rule is shown in Sect. 3.1. See Eqs. (32) and (33) for the expressions as a product rule.

Funded by SCOAP[3]

$\mathcal{N} = 4$ case such that any finite correction to the F-term is prohibited [25]. So we can say that the CLR keeps various natural properties of SUSY at a perturbative level; however, its non-perturbative property, which will be important to extend the CLR formulations to higher dimensions, is still unknown.

In this paper, we propose a lattice action with the CLR for a backward difference operator and study its non-perturbative property using numerical computations. We present a solution of the CLR for any interaction term. Numerical computations are carried out for the ϕ^6 interaction for which SUSY is unbroken. We do not employ the standard Monte Carlo method used in previous studies of SUSY QM [8,17,27–29] but a direct computational method on the basis of a transfer matrix [30,31]; see also Refs. [32–36] for related numerical methods. The obtained energy spectra show that the cut-off dependence of the CLR action is smaller than another lattice action defined by Catterall and Gregory (CG) in Ref. [8]. The numerical results of the SUSY Ward–Takahashi identities (WTIs) also tell us that the full symmetry is restored more rapidly than the CG action for the weak and strong couplings.

This paper is organized as follows. In Sect. 2, we introduce the continuum and the lattice theories of $\mathcal{N} = 2$ SUSY QM. The continuum theory is given in the Euclidean path integral formulation in Sect. 2.1 and the lattice theory is introduced in Sect. 2.2. The CG lattice action is then presented in Sect. 2.3. We formulate the CLR for the backward difference operator showing a solution for any superpotential and mention a relation between the CLR and the standard Leibniz rule in Sect. 3. Section 4 presents the numerical results. In Sect. 4.1, we briefly explain the computational method with the transfer matrix [30]. Then, using computational parameters given in Sect. 4.2, we show the numerical results of energy spectra in Sect. 4.3 and those of SUSY WTIs in Sect. 4.4. We summarize in Sect. 5. Appendix A is devoted to further study of the CLR and Appendix B shows the results of weak coupling expansion of several lattice actions.

2. SUSY QM and the lattice theory

$\mathcal{N} = 2$ supersymmetric quantum mechanics is defined in the Euclidean path integral formulation according to Refs. [22,23,37]. We then present a naive lattice approach to SUSY QM and introduce a known improved lattice action [8].

2.1. $\mathcal{N} = 2$ SUSY QM

With a Euclidean time t, the action of $\mathcal{N} = 2$ SUSY QM is given by

$$S = \int_0^\beta dt \left\{ \frac{1}{2}(\partial_t \phi)^2 + \frac{1}{2} W^2(\phi) + \bar{\psi}\partial_t \psi + \bar{\psi} W'(\phi)\psi \right\}, \tag{1}$$

where $\phi(t)$ is a real bosonic variable and $\bar{\psi}(t), \psi(t)$ are one-component fermionic variables. These variables satisfy the periodic boundary condition such as $\phi(\beta) = \phi(0)$. The superpotential $W(\phi)$ is any function of ϕ, which determines the physical behavior of this model. The partition function is defined as

$$Z_P = \int D\phi D\bar{\psi} D\psi \, e^{-S}, \tag{2}$$

which is the path integral form of the Witten index.

The classical action is invariant under two SUSY transformations,

$$\begin{aligned}\delta\phi &= \epsilon\psi - \bar{\epsilon}\bar{\psi} \\ \delta\psi &= \bar{\epsilon}(\partial_t\phi - W) \\ \delta\bar{\psi} &= -\epsilon(\partial_t\phi + W),\end{aligned} \tag{3}$$

where ϵ and $\bar{\epsilon}$ are global Grassmann parameters. The Leibniz rule is needed to show that the action (1) is invariant under these transformations.

The Witten index Δ is defined by the quantum Hamiltonian $\hat{H}$ as

$$\Delta \equiv \mathrm{Tr}(-1)^{\hat{F}} e^{-\beta\hat{H}} \tag{4}$$

with

$$\hat{H} = \frac{1}{2}\hat{p}^2 + \frac{1}{2}W^2(\hat{q}) + \frac{1}{2}W'(\hat{q})\left[\hat{\psi}^\dagger, \hat{\psi}\right], \tag{5}$$

where $\hat{q}$ and $\hat{p}$ are the position and momentum operators and $\hat{\psi}^\dagger$ and $\hat{\psi}$ are the creation and annihilation operators, which satisfy $[\hat{p}, \hat{q}] = -i$ and $\{\hat{\psi}, \hat{\psi}^\dagger\} = 1$. Here $\hat{F} \equiv \hat{\psi}^\dagger\hat{\psi}$ is the fermion number operator. The trace is a summation over all possible normalized states of the system.

We can also write

$$\Delta = \mathrm{Tr}(e^{-\beta\hat{H}_-}) - \mathrm{Tr}(e^{-\beta\hat{H}_+}), \tag{6}$$

where $\hat{H}_\pm = \frac{1}{2}\hat{p}^2 + \frac{1}{2}W^2(\hat{q}) \pm \frac{1}{2}W'(\hat{q})$ are the Hamiltonians of bosonic $(-)$ and fermionic $(+)$ sectors, respectively. The Witten index does not depend on β because all non-zero eigenmodes form pairs between $\hat{H}_+$ and $\hat{H}_-$ and only β-independent zero modes contribute to Δ. It is well known that Δ is zero (non-zero) when SUSY is broken (unbroken) in this model. We study a SUSY unbroken case with $\Delta = 1$, given by $W(\phi) \simeq \lambda\phi^3$ for $|\phi| \to \infty$, in this paper.

2.2. Lattice theory

The lattice theory is defined on a lattice whose coordinate is given by $t = na\,(n \in \mathbb{Z})$ where a is the lattice spacing. Lattice bosonic and fermionic variables, which live on the sites, are expressed as ϕ_n and ψ_n, respectively. The lattice size N is a positive integer and $\beta = Na$. It is assumed that all variables satisfy the periodic boundary condition

$$\phi_{n+N} = \phi_n, \qquad \psi_{n+N} = \psi_n, \qquad \bar{\psi}_{n+N} = \bar{\psi}_n. \tag{7}$$

The partition function with a lattice action S is given by the same form as Eq. (2) with well-defined measures:

$$\int D\phi \equiv \prod_{n=1}^{N} \int_{-\infty}^{\infty} \frac{d\phi_n}{\sqrt{2\pi a}}, \tag{8}$$

$$\int D\bar{\psi}D\psi \equiv \int \prod_{n=1}^{N} d\bar{\psi}_n d\psi_n. \tag{9}$$

Here each Grassmann measure is an anti-commuting derivative as $d\psi_n \equiv \partial/\partial\psi_n$ and $d\bar{\psi}_n \equiv \partial/\partial\bar{\psi}_n$.

The difference operator ∇ acts on a lattice variable φ_n as $\nabla\varphi_n \equiv \sum_{m\in\mathbb{Z}} \nabla_{nm}\varphi_m$ and its transpose is $(\nabla^T)_{nm} \equiv \nabla_{mn}$. Throughout this paper, ∇_+ and ∇_- denote a simple forward and a backward difference operator, respectively:

$$\nabla_+\varphi_n \equiv \frac{\varphi_{n+1} - \varphi_n}{a}, \tag{10}$$

$$\nabla_-\varphi_n \equiv \frac{\varphi_n - \varphi_{n-1}}{a}. \tag{11}$$

Note that $(\nabla_+)^T = -\nabla_-$.

We now consider a naive lattice action,

$$S_{\text{naive}} = a\sum_n \left\{\frac{1}{2}(\nabla_-\phi_n)^2 + \frac{1}{2}W^2(\phi_n) + \bar{\psi}_n\nabla_-\psi_n + \bar{\psi}_n W'(\phi_n)\psi_n\right\}, \tag{12}$$

which is obtained by replacing $\phi(t)$, $\psi(t)$, $\bar{\psi}(t)$, and ∂_t of Eq. (1) by the corresponding lattice variables ϕ_n, ψ_n, $\bar{\psi}_n$, and ∇_- and replacing the integral by a summation over the lattice site. The summation in Eq. (12) is taken from 1 to N; hereafter the summation with a lattice site n means $\sum_{n=1}^N$ as well. This action is not invariant under a naive lattice SUSY transformation defined by the same replacement of the variables for Eq. (3).

SUSY, which is broken at $\mathcal{O}(a)$ in Eq. (12), is classically restored in the continuum limit $a \to 0$; however, such a restoration does not occur at the quantum level. As seen in later sections, modifying $\mathcal{O}(a)$ interactions of the lattice action, we can keep only one of the two SUSY transformations parametrized by ϵ and $\bar{\epsilon}$ at a finite lattice spacing, and the full symmetry is restored in the quantum continuum limit for such a lattice model.

2.3. Catterall–Gregory lattice model

An improved lattice action, which keeps some symmetries, is proposed by Catterall and Gregory [8]:

$$S_{\text{CG}} = S_{\text{naive}} + a\sum_n \nabla_-\phi_n W(\phi_n), \tag{13}$$

where ∇_- is the backward difference operator defined in Eq. (11). Note that the added term is a kind of surface term that vanishes in the naive continuum limit.

We can show that, in the free limit given by $W(\phi) = ma\phi$, S_{CG} is invariant under the lattice SUSY transformations:

$$\begin{aligned}
\delta\phi_n &= \epsilon\psi_n - \bar{\epsilon}\bar{\psi}_n \\
\delta\psi_n &= \bar{\epsilon}(\nabla_+\phi_n - W(\phi_n)) \\
\delta\bar{\psi}_n &= -\epsilon(\nabla_-\phi_n + W(\phi_n)).
\end{aligned} \tag{14}$$

For interacting cases, it is not invariant under the whole transformations (14) but invariant under part of SUSY, $\delta_\epsilon = \delta|_{\bar{\epsilon}=0}$:

$$\delta_\epsilon S_{\text{CG}} = 0. \tag{15}$$

This is because the extra term on the right-hand side in Eq. (13) provides $-\delta_\epsilon S_{\text{naive}}$ for any finite lattice spacing. The remaining $\bar{\epsilon}$ symmetry in Eq. (14) is restored in the quantum continuum limit as shown in Refs. [8,17,27,30] and also in Sect. 4.4 of this paper.

3. Cyclic Leibniz rule for the backward difference operator

We propose an alternative lattice action with the cyclic Leibniz rule (CLR) for the backward difference operator and show a solution of the CLR for any superpotential. It is straightforward to extend the results to the case of the forward difference operator.

3.1. Lattice action with the CLR

The CLR for the symmetric difference operator is proposed in Ref. [21]. As an straightforward extension of Ref. [21], we introduce a lattice action with the CLR for the backward operator:

$$S_{\text{CLR}} = a\sum_n \left\{\frac{1}{2}(\nabla_-\phi_n)^2 + \frac{1}{2}(W_n)^2 + \bar{\psi}_n\nabla_-\psi_n + \sum_m \bar{\psi}_n W'_{nm}\psi_m\right\}, \tag{16}$$

where W_n is a local function of the boson variables[2] and $W'_{nm} \equiv \frac{\partial W_n}{\partial \phi_m}$. We now assume that W_n satisfies the CLR:

$$\sum_n \left\{W_n(\nabla_-)_{nm} + \nabla_-\phi_n W'_{nm}\right\} = 0. \tag{17}$$

As explained in the next section, a desirable local solution of Eq. (17) is

$$W_n = \frac{U(\phi_n) - U(\phi_{n-1})}{\phi_n - \phi_{n-1}}, \tag{18}$$

where $U(\phi) = \int^\phi d\phi'\, W(\phi')$. The lattice action (16) classically reproduces the continuum one (1) as $a \to 0$ since $W_n = W(\phi_n) + \mathcal{O}(a)$.

The importance of CLR is understood by considering a half lattice SUSY transformation:

$$\begin{aligned}
\delta_\epsilon\phi_n &= \epsilon\psi_n \\
\delta_\epsilon\psi_n &= 0 \\
\delta_\epsilon\bar{\psi}_n &= -\epsilon(\nabla_-\phi_n + W_n).
\end{aligned} \tag{19}$$

The lattice action (16) with any solution of Eq. (17) is invariant under Eq. (19) because

$$\delta_\epsilon S_{\text{CLR}} = \epsilon a\sum_m X_m\psi_m = 0, \tag{20}$$

where

$$X_m \equiv -\sum_n \left\{W_n(\nabla_-)_{nm} + W'_{nm}\nabla_-\phi_n\right\}, \tag{21}$$

which vanishes as long as W_n satisfies the CLR (17).

[2] Note that $W_n \neq W(\phi_n)$ in general because W_n may contain ϕ_m with $m \neq n$ as long as the correlation rapidly vanishes for $|m-n| \to \infty$. See Eq. (A.5) of Appendix A.2 for the strict definition of the locality condition.

The other half transformation of $\mathcal{N} = 2$ is broken on the lattice in general, which is restored at the continuum limit as seen in Sect. 4.4. However, in the free theory, it still remains as an exact symmetry because the free lattice action with the solution (18) is invariant under

$$\begin{aligned} \delta_{\bar{\epsilon}}\phi_n &= -\bar{\epsilon}\bar{\psi}_n \\ \delta_{\bar{\epsilon}}\psi_n &= \bar{\epsilon}(\nabla_+\phi_n - W_{n+1}) \\ \delta_{\bar{\epsilon}}\bar{\psi}_n &= 0. \end{aligned} \tag{22}$$

Note that W_{n+1} is used in $\delta_{\bar{\epsilon}}\psi_n$ instead of W_n. We can actually show that

$$\delta_{\bar{\epsilon}} S_{\mathrm{CLR}} = \bar{\epsilon}\left\{ a\sum_n X_n\bar{\psi}_n + a\sum_{n,m} Y_{nm}(W_n\bar{\psi}_m - \bar{\psi}_m\nabla_-\phi_n) + a\sum_{nmk} Z_{nmk}\bar{\psi}_n\bar{\psi}_k\psi_m \right\}, \tag{23}$$

where

$$\begin{aligned} Y_{nm} &\equiv W'_{m\,n-1} - W'_{n\,m} \\ Z_{nmk} &\equiv \frac{\partial^2 W_n}{\partial\phi_k\partial\phi_m}. \end{aligned} \tag{24}$$

Although we have $X_n = 0$ from the CLR, Y_{nm} and Z_{nmk} do not vanish for a generic superpotential. However, for the free theory with the solution (18),

$$W_n = \frac{m}{2}(\phi_n + \phi_{n-1}), \tag{25}$$

it is easy to show that Y_{mn}, Z_{nmk}, and Eq. (23) vanish.

3.2. A solution of CLR for the backward difference operator

We show that Eq. (18) is a local and well-defined solution of Eq. (17) for a generic superpotential. Once the solution is given, the lattice CLR action retains an exact SUSY as seen in the previous section.

Let us first consider the free theory. For the backward operator $(a\nabla_-)_{nm} = \delta_{nm} - \delta_{n-1,m}$, we take an ansatz solution within the nearest-neighbor interactions, $W_n = d_0\phi_n + d_1\phi_{n-1} + d_2\phi_{n+1}$, $d_0 + d_1 + d_2 = 1$, $d_i \in \mathbb{C}$. It is then found that $d_0 = d_1 = 1/2$, $d_2 = 0$ is a solution of Eq. (17), for which Eq. (25) is obtained. However, this straightforward technique is awkward for a generic superpotential.

Another representation of Eq. (17) makes it easy to find a solution. Rescaling ϕ_n of Eq. (17) as $u\phi_n$ with a parameter $u \in [0, 1]$ and using the chain rule for ∂_u, we obtain

$$\frac{\partial}{\partial u}\sum_n \left\{ u(\nabla_-\phi)_n W_n|_{\phi\to u\phi} \right\} = 0. \tag{26}$$

Integrating Eq. (26) from $u = 0$ to $u = 1$, we find a condition that means a vanishing surface term:

$$\sum_n (\nabla_-\phi)_n W_n = 0. \tag{27}$$

This condition is equivalent to Eq. (17) because Eq. (17) can also be derived from Eq. (27) differentiating Eq. (27) with respect to ϕ_m.

The relation (27) is easily solved by a local function (18). All we have to do is check whether or not W_n given by Eq. (18) is a well-defined function that coincides with $W(\phi_n)$ as $a \to 0$. By integrating $\partial_u U(\phi_n - ua\nabla_-\phi_n)$ from $u = 0$ to $u = 1$, we have

$$U(\phi_n) - U(\phi_{n-1}) = (\phi_n - \phi_{n-1}) \int_0^1 du\, W(\phi_n - au\nabla_-\phi_n). \tag{28}$$

The division in Eq. (18) is well defined because the integral on the right-hand side is well defined for any configuration of ϕ_m. Since the integral is $W(\phi_n)$ up to $\mathcal{O}(a)$, we can immediately show that $W_n = W(\phi_n) + \mathcal{O}(a)$.

3.3. CLR versus Leibniz rule

The difference between the CLR and the standard Leibniz rule (LR) is discussed here. In the continuum theory, LR for ∂_t is $\partial_t W(\phi) = W'(\phi)\partial_t\phi$. So a naive lattice LR is introduced as

$$\text{LR}: \quad \sum_m \{\nabla_{nm} W_m - W'_{nm}\nabla\phi_m\} = 0, \tag{29}$$

for W_n that is a local function of bosonic variables. Here we again use $W'_{nm} \equiv \partial W_n/\partial\phi_m$. We find that the CLR is different from the LR in general since

$$\text{CLR}: \quad \sum_m \{-\nabla^T_{nm} W_m - W'_{mn}\nabla\phi_m\} = 0. \tag{30}$$

Note that W' in the second term is transposed.

The CLR coincides with the LR if $W'_{nm} = W'_{mn}$ for $\nabla^T = -\nabla$ (symmetric difference operators), which corresponds to the case in which the lattice action is invariant under both SUSY transformations [21]. However, the no-go theorem [2] tells us that the LR does not hold for any difference operator and any interacting cases with keeping the locality principle. It is therefore difficult to realize the full SUSY transformation exactly on the lattice. The CLR cannot be realized with a non-trivial solution in this case.

A similar argument holds for the backward difference operator ∇_-. Suppose that W_n is a solution of the CLR and $\delta_{\bar\epsilon} S = 0$. Using $W'_{mn} = W'_{n,m-1}$ from $Y_{nm} = 0$, we can show that the CLR coincides with the LR for ∇_+ since $\nabla^T_- = -\nabla_+$ and $\sum_m W'_{mn}(\nabla_-\phi)_m = \sum W'_{nm}(\nabla_+\phi)_m$. The no-go theorem again tells us that one cannot find a solution of the CLR, for which the lattice action (16) is invariant under both δ_ϵ and $\delta_{\bar\epsilon}$.

The lattice rules (29) and (30) can also be expressed as a product rule of lattice variables. As an example, let us consider a lattice superpotential,

$$W_n^{\text{e.g.}} \equiv \sum_{m,k} M_{nmk}\phi_m\phi_k, \tag{31}$$

as a discretization of $W^{\text{e.g.}}(\phi(x)) = \phi^2(x)$. Then the (two-body) LR can be expressed as

$$\sum_n \Big\{\nabla_{na} M_{bnc} - \nabla_{bn} M_{nca} + \nabla_{nc} M_{ban}\Big\} = 0, \tag{32}$$

while the (two-body) CLR is

$$\sum_n \Big\{\nabla_{na} M_{nbc} + \nabla_{nb} M_{nca} + \nabla_{nc} M_{nab}\Big\} = 0. \tag{33}$$

The name of the *cyclic* Leibniz rule comes from the cyclicity of the indices a, b, c. In Appendix A, an explicit solution for the m-body CLR is also given.

4. Numerical results

Numerical computation is carried out for the CLR action (16) with the periodic boundary condition for the superpotential,

$$W(\phi) = m\phi + \lambda m^2 \phi^3, \tag{34}$$

where λ is the dimensionless coupling constant and m is the mass. Supersymmetry is kept unbroken since the Witten index is non-zero for this potential. The energy spectra and the SUSY Ward–Takahashi identities are evaluated at two coupling constants $\lambda = 0.001$ (weak) and $\lambda = 1$ (strong). We compare the results with those obtained from the CG action (13) to understand the dependence of the results on the lattice spacing.

4.1. Numerical methods

We begin with giving the CLR lattice action used in the actual computations:

$$S_{\mathrm{CLR}} = a \sum_n \left\{ \frac{1}{2}(\nabla_- \phi_n)^2 + \frac{1}{2}(W_n)^2 + \bar{\psi}_n \nabla_- \psi_n + \sum_m \bar{\psi}_n W'_{nm} \psi_m \right\}, \tag{35}$$

where

$$W_n = \frac{ma}{2}(\phi_n + \phi_{n-1}) + \frac{(ma)^2\lambda}{4}(\phi_n^3 + \phi_n^2\phi_{n-1} + \phi_n\phi_{n-1}^2 + \phi_{n-1}^3), \tag{36}$$

$$W'_{nm} = A(\phi_n, \phi_{n-1})\,\delta_{n,m} + A(\phi_{n-1}, \phi_n)\,\delta_{n-1,m}, \tag{37}$$

with

$$A(\alpha, \beta) \equiv \frac{ma}{2} + \frac{(ma)^2\lambda}{4}(3\alpha^2 + 2\alpha\beta + \beta^2). \tag{38}$$

As shown in Sect. 3.1, the action (35) is invariant under a single SUSY transformation (19) thanks to the CLR (17).

It it straightforward to show that, integrating out the fermionic variables, the partition function (2) with Eq. (35) is given as

$$Z_P = \int D\phi \left\{ \prod_{n=1}^{N} (1 + A(\phi_n, \phi_{n-1}))e^{-\mathcal{L}(\phi_n, \phi_{n-1})} - (\phi_n \leftrightarrow \phi_{n-1}, A \to -A) \right\}, \tag{39}$$

where

$$\mathcal{L}(\alpha, \beta) \equiv \frac{1}{2}(\alpha - \beta)^2 + \frac{1}{8}\left(ma(\alpha + \beta) + \frac{(ma)^2\lambda}{2}(\alpha^3 + \alpha^2\beta + \alpha\beta^2 + \beta^3) \right)^2, \tag{40}$$

because $S_B = \sum_{n=1}^{N} \mathcal{L}(\phi_n, \phi_{n-1})$. Note that $A(\alpha, \beta)$ and $\mathcal{L}(\alpha, \beta)$ are infinite-dimensional matrices since $\alpha, \beta \in \mathbb{R}$.

The partition function and the correlation functions are expressed in terms of transfer matrices. In order to define finite-dimensional matrices, each path integral of Eq. (39) is discretized by a

quadrature. The Gauss–Hermite quadrature formula is given by an approximation of the integral of a function $f(x)$:

$$\int_{-\infty}^{\infty} dx f(x) \approx \sum_{x \in S_K} g_K(x) f(x), \tag{41}$$

where S_K is a set of roots of the Kth Hermite polynomial H_K and the weight $g_K(x)$ is

$$g_K(x) = \frac{2^{K-1} K! \sqrt{\pi}}{K^2 H_{K-1}^2(x)} e^{x^2}. \tag{42}$$

Since K is the order of the approximation, the sum of Eq. (41) is expected to reproduce the integral on the left-hand side as $K \to \infty$. We will check the convergence of the quadrature, which depends on the details of the action, by observing the K dependence of the numerical results.

We can express Z_P using finite-dimensional matrices $T_\pm$ as

$$Z_P \approx \mathrm{tr}(T_-^N) - \mathrm{tr}(T_+^N), \tag{43}$$

where, for $\alpha, \beta \in S_K$,

$$(T_-)_{\alpha\beta} \equiv (1 + A(\alpha, \beta)) R_{\alpha\beta}, \tag{44}$$

$$(T_+)_{\alpha\beta} \equiv (1 - A(\beta, \alpha)) R_{\alpha\beta}, \tag{45}$$

$$R_{\alpha\beta} \equiv \sqrt{\frac{g_K(\alpha) g_K(\beta)}{2\pi}}\, e^{-\mathcal{L}(\alpha,\beta)}, \tag{46}$$

discretizing all path integral measures (8) by the Gauss–Hermite quadrature (41). A comparison with Eq. (6) tells us that T_- and T_+ are a bosonic and fermionic transfer matrix, respectively. The trace of Eq. (43) means

$$\mathrm{tr}(X) \equiv \sum_{\alpha \in S_K} X_{\alpha\alpha}, \tag{47}$$

where $X_{\alpha\beta}$ is a matrix with $\alpha, \beta \in S_K$.

Similarly, any correlation function is given in terms of the transfer matrices. We basically follow Ref. [30] to derive the expressions. The two-point correlation function of the bosonic variable is

$$\langle \phi_j \phi_k \rangle \approx \frac{1}{Z} \mathrm{Tr} \left\{ T_-^{N-k+j} D T_-^{k-j} D - T_+^{N-j+k} D T_+^{k-j} D \right\}, \tag{48}$$

for $0 \le j \le k \le N$. Here D, defined as

$$D_{\alpha\beta} \equiv \alpha \delta_{\alpha\beta}, \tag{49}$$

represents an operator insertion. The boson two-point function is exactly the same formula as that of the CG action [30]. On the other hand, the fermion two-point function is slightly different:

$$\langle \psi_j \bar{\psi}_k \rangle \approx \frac{1}{Z} \mathrm{tr} \left\{ R T_-^{k-j-1} T_+^{N+j-k} \right\}, \tag{50}$$

for $0 \le j \le k \le N$.[3]

[3] The formula for the CG action given in Ref. [30] is properly reproduced because $T_+ = R$ in this case.

The transfer matrices $T_\pm$ can be improved by rescaling the bosonic variables before the discretization of the measures. According to Ref. [30], applying the quadrature after rescaling ϕ as $\phi \to \phi/s$ ($s \in \mathbb{R}$), we have

$$(T_-^{(s)})_{\alpha\beta} \equiv \left(1 + A\left(\alpha s^{-1}, \beta s^{-1}\right)\right) R_{\alpha\beta}^{(s)}, \tag{51}$$

$$(T_+^{(s)})_{\alpha\beta} \equiv \left(1 - A\left(\beta s^{-1}, \alpha s^{-1}\right)\right) R_{\alpha\beta}^{(s)}, \tag{52}$$

$$R_{\alpha\beta}^{(s)} \equiv \sqrt{\frac{g_K(\alpha) g_K(\beta)}{2\pi s^2}}\, e^{-\mathcal{L}(\alpha s^{-1}, \beta s^{-1})}. \tag{53}$$

The partition function and the correlation functions are then given by the same formulas as Eqs. (43), (48), and (50) with $T_\pm^{(s)}$ and $R^{(s)}$ instead of $T_\pm$ and R. The operator insertion D is also replaced by $D^{(s)} = D/s$ while the trace is still given by Eq. (47). We can obtain computational results with high precision by tuning the rescaling parameter s such that the Witten index $Z_P = 1$ is realized as accurately as possible.

4.2. Computational parameters

Table 1 shows the parameters used in our computations of the CLR action. We employ two representative coupling constants, $\lambda = 0.001$ as a weak coupling and $\lambda = 1$ as a strong coupling. The rescaling parameter s should be tuned for each parameter set such that the Witten index $Z_P = 1$ is reproduced as accurately as possible, as done in Ref. [30]. The matrix sizes K used for the SUSY WTIs are smaller than those for the mass spectra to reduce the computational cost. This is because the SUSY WTIs are evaluated by performing the direct matrix product several times while the mass spectra are evaluated by diagonalizing $T_\pm$ once. Similarly, we use the same lattice sizes with a slightly different s for the CG action.

We take $m\beta = 30$, which is large enough to obtain the numerical results with a negligible finite-β effect because $e^{-\beta E_1} < O(10^{-13})$ for the first excited energy $E_1/m \geq 1$. The lattice spacing is shown as a rounded number, which is uniquely determined from the lattice size N for fixed $m\beta$ as $ma = m\beta/N(= 30/N)$. For instance, $ma = 0.017\,964\cdots$ for $N = 1670$ is denoted as $ma = 0.018$ in the table but we use $ma = 30/N$ in the actual computations without loss of digit.

Figure 1 shows the results of Z_P against β for several s. Although $Z_P = 1$ is analytically shown even on the lattice [21], the numerical results depend on β. The deviations from $Z_P = 1$ are systematic errors that come from the finite-K effect. We can decrease the errors tuning s for fixed K. We find that $s = 0.68$ leads to $|Z_P - 1| < O(10^{-9})$ for $K = 150$ in the case of $ma = 0.01$ and $\lambda = 1$. Each parameter has a different value of s so that $Z_P = 1$ is realized within $O(10^{-9})$ as shown in Table 1.

4.3. Energy spectra

The energy spectra are read from two transfer matrices $T_\pm$ associated with two Hamiltonians $\hat{H}_\pm$ as $T_\pm \approx e^{-a\hat{H}_\pm}$. The energy eigenvalues of the bosonic and fermionic states E_n^B and E_n^F are thus obtained from the nth eigenvalue of $T_\pm$: $(T_-)_n = \mathrm{e}^{-aE_n^B}$ and $(T_+)_n = \mathrm{e}^{-aE_n^F}$. We use numerical diagonalizations of $T_\pm$ to evaluate $(T_\pm)_n$. The non-zero eigenvalues are degenerate between $\hat{H}_+$ and $\hat{H}_-$ and only $\hat{H}_-$ has a zero mode for the superpotential (34). We expect that $T_\pm$ have the same spectra even on the lattice thanks to the exact SUSY.

Table 1. Parameters used in the numerical computations of the CLR system. The top and bottom tables are those for a weak coupling $\lambda = 0.001$ and for a strong coupling $\lambda = 1$, respectively.

$\lambda = 0.001$							
Energy spectra				SUSY WTI			
ma	*s*	*N*	*K*	*ma*	*s*	*N*	*K*
0.020	0.47	1500	150	0.600	1.39	50	40
0.019	0.46	1580	150	0.500	1.26	60	40
0.018	0.45	1670	150	0.400	1.13	75	40
0.017	0.44	1770	150	0.300	0.97	100	40
0.016	0.42	1880	150	0.250	0.89	120	40
0.015	0.41	2000	150	0.200	0.79	150	40
0.014	0.40	2140	150	0.150	0.68	200	40
0.013	0.38	2310	150	0.100	0.56	300	40
0.012	0.37	2500	150	0.080	0.51	375	40
0.011	0.36	2730	150	0.060	0.49	500	50
0.010	0.34	3000	150	0.050	0.44	600	50
0.009	0.33	3330	150	0.040	0.44	750	60
0.008	0.33	3750	170	0.030	0.41	1000	70
0.007	0.30	4290	170	0.025	0.34	1200	70
0.006	0.27	5000	170	0.020	0.32	1500	80
0.005	0.27	6000	200	0.015	0.33	2000	100
0.004	0.24	7500	200	0.010	0.29	3000	120

$\lambda = 1$							
Energy spectra				SUSY WTI			
ma	*s*	*N*	*K*	*ma*	*s*	*N*	*K*
0.020	0.97	1500	150	0.600	2.93	50	40
0.019	0.95	1580	150	0.500	2.68	60	40
0.018	0.92	1670	150	0.400	2.46	75	40
0.017	0.90	1770	150	0.300	2.08	100	40
0.016	0.87	1880	150	0.250	1.89	120	40
0.015	0.84	2000	150	0.200	1.69	150	40
0.014	0.81	2140	150	0.150	1.47	200	40
0.013	0.78	2310	150	0.100	1.18	300	40
0.012	0.75	2500	150	0.080	1.06	375	40
0.011	0.72	2730	150	0.060	0.91	500	40
0.010	0.68	3000	150	0.050	0.83	600	40
0.009	0.65	3330	150	0.040	0.74	750	40
0.008	0.61	3750	150	0.030	0.64	1000	40
0.007	0.57	4290	150	0.025	0.65	1200	50
0.006	0.53	5000	150	0.020	0.57	1500	50
0.005	0.48	6000	150	0.015	0.58	2000	70
0.004	0.46	7500	170	0.010	0.47	3000	70
0.003	0.40	10 000	170				
0.002	0.32	15 000	170				
0.001	0.23	30 000	200				

4.3.1. Weak coupling results

Table 2 shows the 10 smallest energy eigenvalues obtained from the CLR action for $\lambda = 0.001$ at a lattice spacing $ma = 0.01$. The central values are those obtained for $K = 150$ and the errors are estimated from the largest difference among the results with $K = 140, 150, \ldots, 200$. The spectra

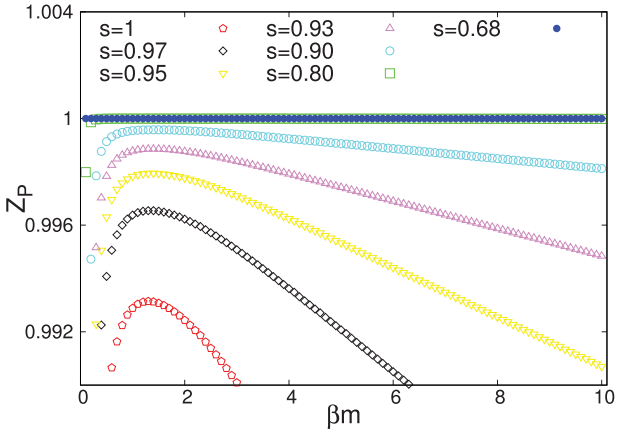

Fig. 1. Partition function with the periodic boundary condition against β for the CLR action. We use several s with fixed $K = 150$ for $ma = 0.01, \lambda = 1$.

Table 2. Energy eigenvalues obtained from the CLR action for $\lambda = 0.001$ at $ma = 0.01$.

n	E_n^B/m	E_n^F/m
0	0.000 000 000 01(3)	
1	1.001 498 936(1)	1.001 498 935 46(2)
2	2.005 980 24(3)	2.005 980 230(1)
3	3.013 4265(5)	3.013 426 35(3)
4	4.023 822(5)	4.023 8202(4)
5	5.037 16(4)	5.037 146(5)
6	6.0535(3)	6.053 40(4)
7	7.073(1)	7.0726(2)
8	8.097(5)	8.095(1)
9	9.13(2)	9.122(5)
10	10.18(4)	10.16(1)

are very similar to those of the harmonic oscillator, $E_n = nm\,(n = 1, 2, \ldots)$, since $\lambda = 0.001$ is small enough. As we expected, E_n^B and E_n^F coincide with each other within the errors. The same degeneracies are observed for the other lattice spacings.

Figure 2 shows the five lowest eigenvalues against the lattice spacing ma. Since the difference between E_n^B and E_n^F is sufficiently smaller than the systematic errors from the finite-K effect, we plotted only E_n^F as E_n in the figure. As we can see, the cut-off dependence of the CLR action is milder than that of the CG action.

Tables 3 and 4 show the fit results of the five lowest energy eigenvalues for the CLR and CG actions, respectively. For the continuum extrapolation, we employ a quadratic polynomial:

$$E/m = a_0 + a_1(ma) + a_2(ma)^2. \tag{54}$$

Two actions reproduce the same a_0, which is E_n/m at the continuum limit, within the errors. The CLR action behaves similarly to the continuum theory in comparison with the CG action as suggested from small values of a_1.

The weak coupling expansion of the first excited energy is demonstrated in Appendix B, in which the quantum corrections to the masses are evaluated from the correlation functions. We find that, for

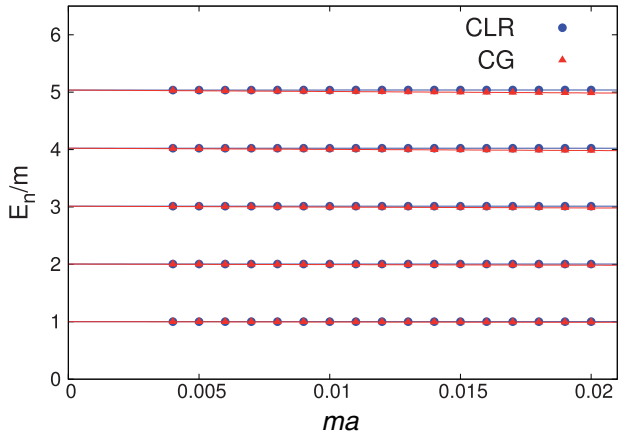

Fig. 2. The five lowest energy eigenvalues against the lattice spacing ma for $\lambda = 0.001$. The results of CLR (circles) show a better convergence than the CG results (triangles). The solid lines represent the fit results shown in Tables 3 and 4.

Table 3. Fit results of E_n for the CLR action with $\lambda = 0.001$.

	E_1/m	E_2/m	E_3/m	E_4/m	E_5/m
a_0	1.001 495 535(1)	2.005 973 34(3)	3.013 4165(4)	4.023 814(4)	5.0372(4)
a_1	−0.000 4999(4)	−0.001 01(1)	−0.0017(2)	−0.004(2)	−0.02(2)
a_2	0.084 00(4)	0.1702(9)	0.27(1)	0.5(2)	2(1)

Table 4. Fit results of E_n for the CG action with $\lambda = 0.001$.

	E_1/m	E_2/m	E_3/m	E_4/m	E_5/m
a_0	1.001 4954(2)	2.005 9732(4)	3.013 4161(9)	4.023 806(1)	5.037 131(3)
a_1	−0.502 21(6)	−1.0089(1)	−1.5202(3)	−2.0357(3)	−2.557(1)
a_2	0.330(3)	0.667(7)	1.02(2)	1.36(2)	1.8(1)

$E_1 \equiv E_1^F = E_1^B$, the one-loop result of the CLR action is

$$\frac{E_1^{\mathrm{CLR}}}{m} = 1 + \frac{3}{2}\lambda - \frac{1}{2}ma\lambda + O((ma)^2, \lambda^2), \tag{55}$$

while that of the CG action is

$$\frac{E_1^{\mathrm{CG}}}{m} = 1 + \frac{3}{2}\lambda - \frac{1}{2}ma - \frac{9}{4}ma\lambda + O((ma)^2, \lambda^2). \tag{56}$$

Both one-loop results coincide with that of the continuum theory, $E^{\mathrm{cont}}/m = 1 + \frac{3}{2}\lambda$, as $a \to 0$. The CG action has a large discretization error due to the third term of $O(ma)$ in Eq. (56), while the $O(a)$ term starts from $O(\lambda ma)$ in the CLR action, which is much smaller than $O(ma)$ for $\lambda = 0.001$.

Figure 3 shows the numerical results of E_1 with the perturbative ones (55) and (56) for $ma \leq 0.02$. The numerical results nicely reproduce the perturbation theory shown by the dotted lines and the relative errors are of the order of 10^{-6}, which is the same size as λ^2. Although a linear ma dependence is seen in the CG results, the CLR results perfectly reproduce the continuum theory for this range of ma since the third term of Eq. (55) is negligibly small for $\lambda = 0.001$.

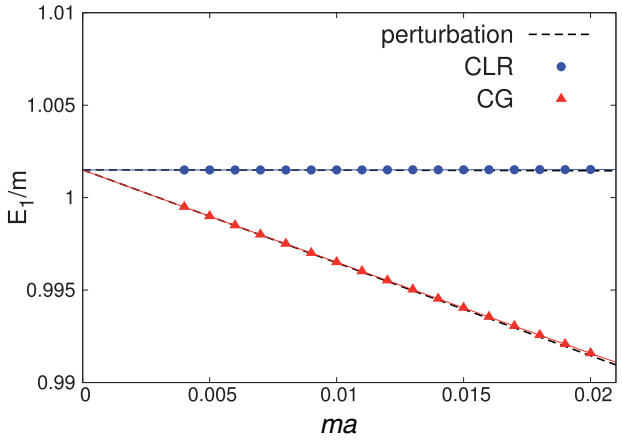

Fig. 3. Continuum limit of E_1 for $\lambda = 0.001$. The solid lines represent the fit results and the dotted lines are the perturbative results

Table 5. Energy eigenvalues obtained from the CLR action for $\lambda = 1$ at $ma = 0.01$.

n	E_n^B/m	E_n^F/m
0	0.000 000 0000(2)	
1	1.682 687 275(2)	1.682 687 274 859(4)
2	4.365 387 624(8)	4.365 387 623 19(6)
3	7.622 118 41(4)	7.622 118 4119(5)
4	11.364 0034(2)	11.364 003 389(3)
5	15.527 3615(7)	15.527 361 44(2)
6	20.068 372(3)	20.068 372 02(9)
7	24.954 588(9)	24.954 5871(4)
8	30.160 73(3)	30.160 725(2)
9	35.666 38(9)	35.666 371(6)
10	41.4546(3)	41.454 59(2)

4.3.2. Strong coupling results

Table 5 shows the 10 smallest energy eigenvalues obtained from the CLR action for $\lambda = 1$ at a fixed $ma = 0.01$. The central values are again those evaluated for $K = 150$ and the errors are estimated from the largest difference among the results for $K = 140, 150, \ldots, 200$. The energy spectra have large quantum corrections compared with Fig. 2 for the weak coupling $\lambda = 0.001$. E_n^B and E_n^F coincide with each other within the errors as well as the case of the weak coupling.

Figure 4 shows the five lowest energy eigenvalues against ma for $\lambda = 1$. We also show Fig. 5, which focuses on E_1 for $\lambda = 1$, for a comparison with Fig. 3. The obtained E_n^F is again plotted as E_n since $E_n^F = E_n^B$ within the sufficiently small errors of $O(10^{-8})$. The cut-off dependence of the CLR action is milder than that of CG action as well as the weak coupling shown in Fig. 2.

Tables 6 and 7 show the fit results of E_n with a quadratic function (54). The same a_0, which is E/m in the continuum limit, is obtained between the CLR and CG actions. As a visible difference between Figs. 2 and 4 is seen, the coefficients a_1 and a_2 are systematically larger than those for the weak coupling, which are shown in Tables 3 and 4. In the strong coupling region, we can confirm that the $O(a)$ dependence of E_1 obtained for the CLR action is still smaller than that of the CG action.

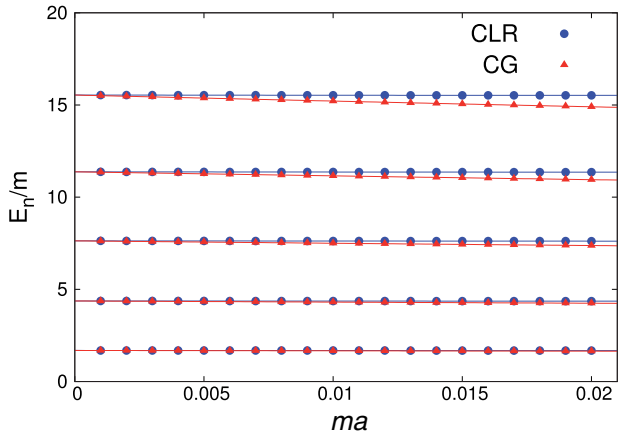

Fig. 4. The five lowest energy eigenstates against ma for $\lambda = 1$. The results of CLR and CG are shown as circles and triangles, respectively. The solid lines represent the fit results shown in Tables 6 and 7.

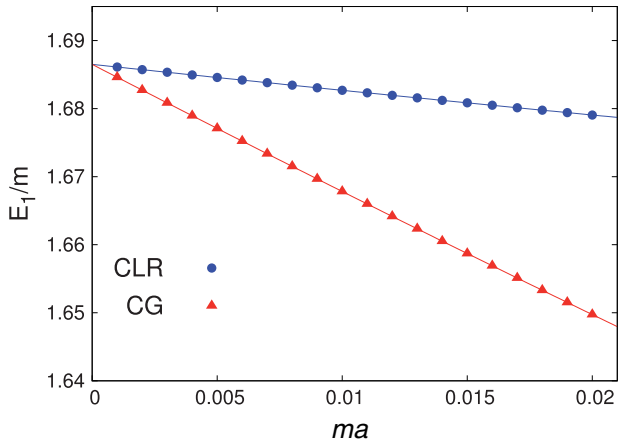

Fig. 5. Continuum limit of E_1 for $\lambda = 1$.

Table 6. Fit results of E_n for the CLR action with $\lambda = 1$.

	E_1/m	E_2/m	E_3/m	E_4/m	E_5/m
a_0	1.686 5004(6)	4.371 816(2)	7.630 953(5)	11.374 845(7)	15.539 78(1)
a_1	−0.3907(3)	−0.684(1)	−0.985(2)	−1.282(3)	−1.575(4)
a_2	0.94(2)	4.08(8)	10.2(2)	19.8(2)	33.3(3)

Table 7. Fit results of E_n for the CG action with $\lambda = 1$.

	E_1/m	E_2/m	E_3/m	E_4/m	E_5/m
a_0	1.686 500(3)	4.371 81(1)	7.630 95(4)	11.374 83(8)	15.5398(1)
a_1	−1.898(1)	−6.422(6)	−13.30(2)	−22.43(3)	−33.75(6)
a_2	3.05(9)	12.6(4)	31(1)	58(5)	95(5)

4.4. SUSY WT identities

The CLR action has an exact SUSY parametrized by ϵ in Eq. (19) while the other $\bar{\epsilon}$ symmetry is broken at finite lattice spacing for any interacting case. The correct mass spectra shown in the

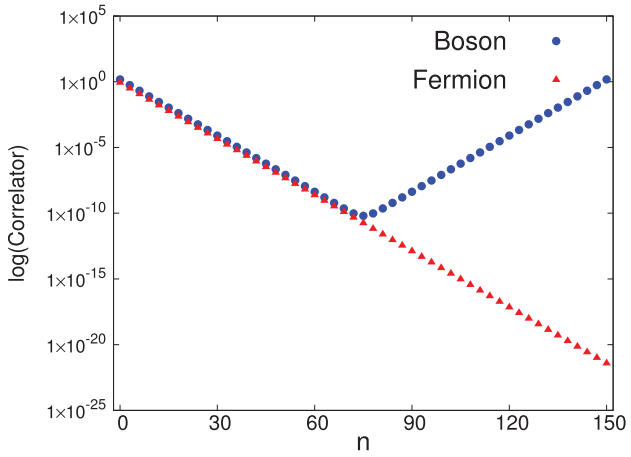

Fig. 6. $\langle \phi_n \phi_N \rangle$ and $\langle \psi_n \bar{\psi}_N \rangle$ obtained from the CLR action for $\lambda = 1$ and $ma = 0.2$. The x-axis denotes the lattice site n and the y-axis shows the numerical values of the correlators on a logarithmic scale.

previous section imply that the broken $\bar{\epsilon}$ symmetry is restored in the continuum limit. Testing the SUSY WTIs, we study the restoration of the full SUSY.

To this end, we first define the SUSY WTIs on the lattice. However, the broken $\bar{\epsilon}$ transformation cannot be uniquely defined on the lattice because one can add any $O(a)$ term to the transformation. Here, for the CLR action, we employ Eq. (22) as a lattice $\bar{\epsilon}$ transformation, which is an exact symmetry in the free theory. Correspondingly, we use Eq. (14) for the CG action, whose $\bar{\epsilon}$ transformation is exactly kept in the free case of Eq. (13).

We can show that

$$\langle \delta(\phi_n \bar{\psi}_N + \psi_n \phi_N) \rangle = \epsilon R_n + \bar{\epsilon} \bar{R}_n, \tag{57}$$

where

$$R_n \equiv \langle \psi_n \bar{\psi}_N \rangle - \langle \phi_n (\nabla_- \phi)_N \rangle - \langle \phi_n W_N \rangle, \tag{58}$$

$$\bar{R}_n \equiv \langle \psi_n \bar{\psi}_N \rangle - \langle \phi_n (\nabla_- \phi)_N \rangle - \langle W_{n+1} \phi_N \rangle, \tag{59}$$

for the CLR action. For the CG action, W_N and W_{n+1} of Eqs. (58) and (59) are replaced by $W(\phi_N)$ and $W(\phi_n)$, respectively. The second term of $\bar{R}_n$ is actually found as $\langle (\nabla_+ \phi)_n \phi_N \rangle$, which can be written in the same form as the second term of R_n using the translational invariance. Note that the third term is the only difference between R_n and $\bar{R}_n$.

For any interacting case, we have $R_n = 0$ since the ϵ transformation is an exact symmetry of the lattice actions. However, $\bar{R}_n$ does not vanish at any finite lattice spacing for the interacting cases even if it vanishes for the free theory. If the $\bar{\epsilon}$ symmetry is restored at a quantum continuum limit, $\bar{R}_n$ should approach zero as $a \to 0$. We evaluate $\bar{R}_n$ numerically to confirm whether the second SUSY WTI holds in the continuum limit or not, as already investigated for the CG action in Refs. [17,27,30].

Figure 6 shows $\langle \phi_n \phi_N \rangle$ and $\langle \psi_n \bar{\psi}_N \rangle$ for $\lambda = 1$ and $ma = 0.2$. When N is sufficiently large, as confirmed in the figure, $\langle \phi_n \phi_N \rangle$ and $\langle \psi_n \bar{\psi}_N \rangle$ behave as

$$\langle \phi_n \phi_N \rangle \approx C(e^{-anE_1} + e^{-a(N-n)E_1}), \tag{60}$$

$$\langle \psi_n \bar{\psi}_N \rangle \approx De^{-anE_1}, \tag{61}$$

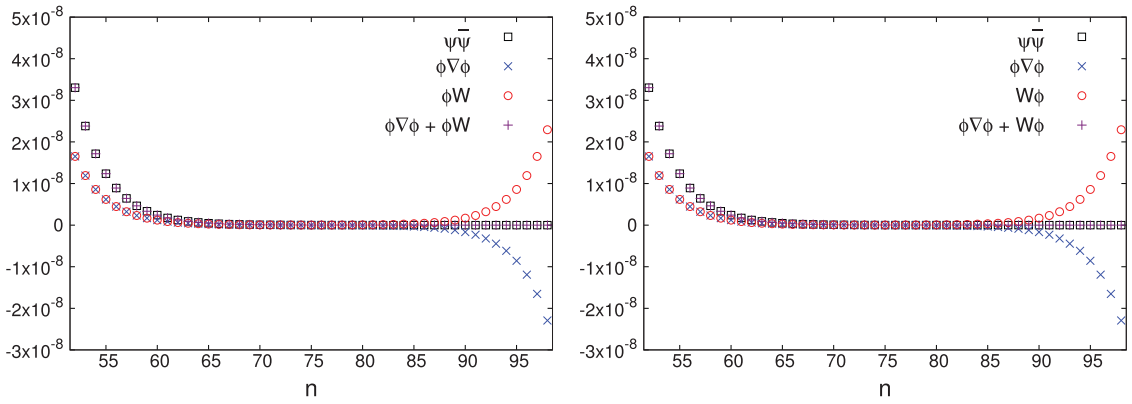

Fig. 7. Three correlation functions in R_n (left) and $\bar{R}_n$ (right) for the CLR action. The cancellations among them are clearly observed.

for $1 \ll n \ll N$. Here C and D are some constants that depend on the lattice spacing. Similarly, using the translational invariance, the other correlation functions in R_n and $\bar{R}_n$ are expected to be

$$\langle \phi_n \nabla_- \phi_N \rangle \approx C_1 (e^{-anE_1} - e^{-a(N-n-1)E_1}), \tag{62}$$

$$\langle \phi_n W_N \rangle \approx C_2 e^{-anE_1} + C_3 e^{-a(N-n-1)E_1}, \tag{63}$$

$$\langle W_{n+1} \phi_N \rangle \approx C_3 e^{-anE_1} + C_2 e^{-a(N-n-1)E_1}, \tag{64}$$

for $1 \ll n \ll N$. Here $C_1 = C(1 - e^{-aE_1})/a$ and C_2, C_3 are some constants that depend on the lattice spacing. Note that it is possible to ignore the contribution from the second excited state for $1 \ll n \ll N$. We can immediately show that

$$C_1 = C_3 = D - C_2 \tag{65}$$

from $R_n = 0$ and the second WTI holds if and only if $C_2 \to C_3$ as $a \to 0$.

Figure 7 shows the cancellation among three correlation functions in R_n (left) and $\bar{R}_n$ (right) for $\lambda = 1$ and $ma = 0.2$. In Fig. 8, similar plots are shown for the CG action. As we expected, the other correlators show the behavior of Eqs. (62), (63), and (64). The cancellation for $n < N/2$ is realized in a different way from that of $n > N/2$. As suggested from Eqs. (61)–(64), the sum of two bosonic correlators (denoted as crosses) cancels the fermion correlator (denoted as squares) for $1 \ll n \ll N/2$ while two bosonic correlators cancel each other out for $N/2 \ll n \ll N$ since the fermion correlator is approximately zero compared with the others.

Since each term of R_n and $\bar{R}_n$ is very small for $n \simeq N/2$, we normalize them to observe the breaking effect clearly:

$$S_n \equiv \frac{R_n}{|\langle \psi_n \bar{\psi}_N \rangle| + |\langle \phi_n (\nabla_- \phi)_N \rangle| + |\langle \phi_n W_N \rangle|} \tag{66}$$

$$\bar{S}_n \equiv \frac{\bar{R}_n}{|\langle \psi_n \bar{\psi}_N \rangle| + |\langle \phi_n (\nabla_- \phi)_N \rangle| + |\langle W_{n+1} \phi_N \rangle|}. \tag{67}$$

Note again that W_N and W_{n+1} of Eqs. (66) and (67) are replaced by $W(\phi_N)$ and $W(\phi_n)$, respectively, for the CG action. It is immediately found that $S_n = 0$ for any n since $R_n = 0$.

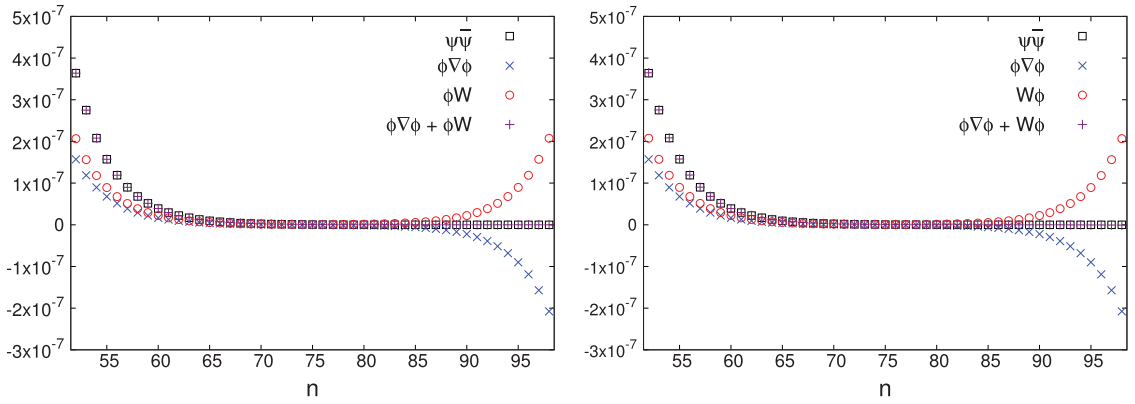

Fig. 8. Three correlation functions in R_n (left) and $\bar{R}_n$ (right) for the CG action. The cancellations are observed as well as the CLR case shown in Fig. 7.

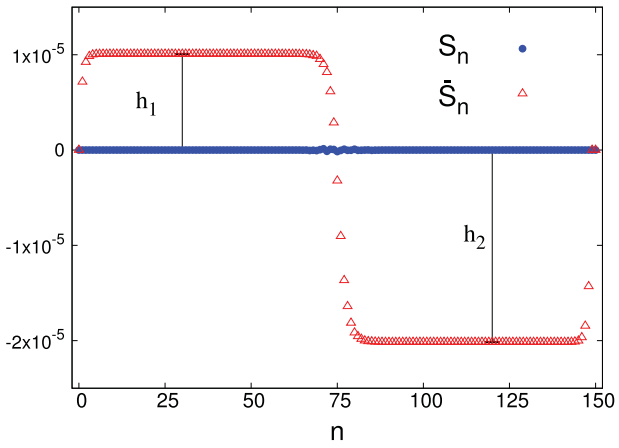

Fig. 9. S_n and $\bar{S}_n$ for the CLR action with $\lambda = 1$ and $ma = 0.2$.

The asymptotic behavior of $\bar{S}_n$ can be understood from Eqs. (61), (62), and (64). For sufficiently large N, it can be shown that $\bar{S}_n$ behaves as constants:

$$S_n \approx h_1 \equiv \frac{C_2 - C_3}{2|C_3| + |D|}, \qquad (1 \ll n \ll N/2) \tag{68}$$

and

$$S_n \approx h_2 \equiv \frac{C_3 - C_2}{|C_2| + |C_3|}, \qquad (N/2 \ll n \ll N). \tag{69}$$

We have

$$h_2 = -2h_1 + O(h_1^2), \tag{70}$$

when C_2 and C_3 have the same sign. Similar identities to Eqs. (68), (69), and (70) hold for the CG action.

In Figs. 9 and 10, S_n and $\bar{S}_n$ are plotted against n. Obviously, S_n vanishes as the numerical results while $\bar{S}_n$ has two plateaux corresponding to h_1 and h_2. We should note that the scale of the y-axis for the CLR action is rather smaller than that of the CG action. The value of $\bar{S}_n$ rapidly changes from h_1 to h_2 around $n = N/2$ as a result of the cancellation of the three correlation functions.

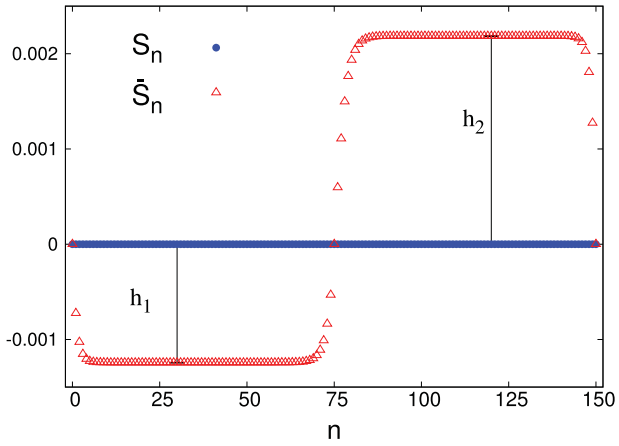

Fig. 10. S_n and $\bar{S}_n$ for the CG action with $\lambda = 1$ and $ma = 0.2$.

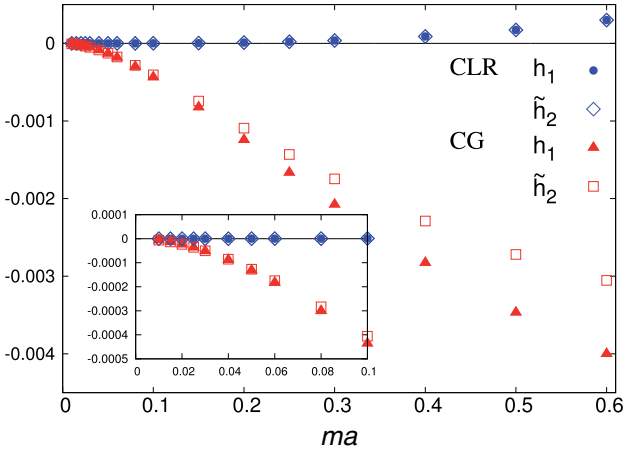

Fig. 11. Lattice spacing dependence of h_1 and h_2 for $\lambda = 1$. We plot h_1 and $\tilde{h}_2 = -h_2/2$, which are evaluated at $n = N/5$ and $n = 4N/5$, as circles and diamonds for the CLR action and triangles and squares for the CG action.

Figure 11 shows the lattice spacing dependence of h_1 and h_2 for $\lambda = 1$ and the numerical values are shown in Table 8 for the convenience of further studies. Figure 12 shows the same plot for $\lambda = 0.001$. We evaluate h_1 and h_2 at $n = N/5$ and $n = 4N/5$, respectively. It can be seen that h_1 and h_2 approach zero as $a \to 0$. Consequently, the second SUSY WTI holds in the continuum limit, i.e., full SUSY is restored in the quantum continuum limit in the low-energy region $1 \ll n \ll N$. The breaking effects h_1 and h_2 of the CLR action are significantly smaller than the CG action even for the strong coupling. Thus we can conclude that the CLR shows a good behavior that is similar to the continuum theory at a non-perturbative level.

5. Summary and discussion

The property of the cyclic Leibniz rule has been studied in $\mathcal{N} = 2$ SUSY QM beyond the perturbation theory. We have defined the lattice action on the basis of the CLR with the backward difference operator giving a solution for any superpotential. The numerical computations have been carried out using the transfer matrix representation of the partition function and the correlation functions. Tuning

Table 8. Numerical values of h_1 and h_2 for $\lambda = 1$.

	CLR		CG	
ma	h_1	h_2	h_1	h_2
0.600	$2.993\,917\,82(7)\times10^{-4}$	$-5.986\,0435(2)\times10^{-4}$	$-4.001\,2296(2)\times10^{-3}$	$6.107\,593\,35(1)\times10^{-3}$
0.500	$1.727\,581(1)\times10^{-4}$	$-3.454\,565(2)\times10^{-4}$	$-3.468\,6833(2)\times10^{-3}$	$5.440\,243\,40(3)\times10^{-3}$
0.400	$8.8385(4)\times10^{-5}$	$-1.7675(1)\times10^{-4}$	$-2.828\,3733(2)\times10^{-3}$	$4.578\,249\,26(3)\times10^{-3}$
0.300	$3.667\,16(2)\times10^{-5}$	$-7.33404(4)\times10^{-5}$	$-2.077\,5005(1)\times10^{-3}$	$3.490\,8132(8)\times10^{-3}$
0.250	$2.068\,870(6)\times10^{-5}$	$-4.13765(1)\times10^{-5}$	$-1.666\,9089(1)\times10^{-3}$	$2.861\,5897(1)\times10^{-3}$
0.200	$1.008\,226(2)\times10^{-5}$	$-2.01643(1)\times10^{-5}$	$-1.243\,420\,44(8)\times10^{-3}$	$2.185\,8056(1)\times10^{-3}$
0.150	$3.871\,90(2)\times10^{-6}$	$-7.7438(4)\times10^{-6}$	$-8.236\,2334(4)\times10^{-4}$	$1.486\,6210(1)\times10^{-3}$
0.100	$9.512\,90(6)\times10^{-7}$	$-1.90258(8)\times10^{-6}$	$-4.365\,2327(1)\times10^{-4}$	$8.116\,901(1)\times10^{-4}$
0.080	$4.2875(1)\times10^{-7}$	$-8.575(1)\times10^{-7}$	$-3.010\,5156(6)\times10^{-4}$	$5.671\,0394(7)\times10^{-4}$
0.060	$1.501\,27(2)\times10^{-7}$	$-3.003(1)\times10^{-7}$	$-1.830\,1692(4)\times10^{-4}$	$3.495\,123(2)\times10^{-4}$
0.050	$7.6345(2)\times10^{-8}$	$-1.527(1)\times10^{-7}$	$-1.322\,9006(2)\times10^{-4}$	$2.544\,4813(8)\times10^{-4}$
0.040	$3.3033(3)\times10^{-8}$	$-6.607(1)\times10^{-8}$	$-8.820\,5996(4)\times10^{-5}$	$1.709\,075(1)\times10^{-4}$
0.030	$1.1062(6)\times10^{-8}$	$-2.21(2)\times10^{-8}$	$-5.174\,1110(6)\times10^{-5}$	$1.010\,147(1)\times10^{-4}$
0.025	$5.49(2)\times10^{-9}$	$-1.10(4)\times10^{-8}$	$-3.670\,7175(4)\times10^{-5}$	$7.194\,15(1)\times10^{-5}$
0.020	$2.318(6)\times10^{-9}$	$-4.6(1)\times10^{-9}$	$-2.400\,6488(8)\times10^{-5}$	$4.723\,49(1)\times10^{-5}$
0.015	$7.56(4)\times10^{-10}$	$-1.5(4)\times10^{-9}$	$-1.380\,3022(8)\times10^{-5}$	$2.726\,72(4)\times10^{-5}$
0.010	$1.5(1)\times10^{-10}$	$-3(1)\times10^{-10}$	$-6.272\,57(1)\times10^{-6}$	$1.244\,15(2)\times10^{-5}$

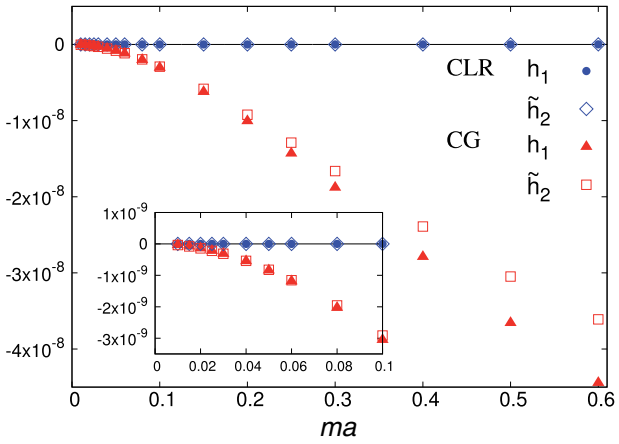

Fig. 12. Lattice spacing dependence of h_1 and h_2 for $\lambda = 0.001$. We plot h_1 and $\tilde{h}_2 = -h_2/2$, which are evaluated at $n = N/5$ and $n = 4N/5$, as circles and diamonds for the CLR action and triangles and squares for the CG action.

the rescaling parameter, the energy spectra and SUSY Ward–Takahashi identities are obtained to high accuracy. We have compared them with those of the Catterall–Gregory action.

Although the number of exact symmetry is the same between the CLR and the CG actions, the CLR action provides a milder cut-off dependence of energy spectra for both weak and strong couplings. In the weak coupling limit, the $\mathcal{O}(a)$ term does not appear in the energy spectra for the CLR action but does for the CG action. Even for the strong coupling, we have observed that the coefficient of the $\mathcal{O}(a)$ term for the CLR action is smaller than the CG action. The lattice SUSY WTIs have shown the same tendency in the cut-off behavior.

There is a wider class of solutions for the CLR and actually Refs. [21,24] investigated it for a symmetric difference operator. By using a different solution, there is a possibility of eliminating an

$\mathcal{O}(a)$ SUSY breaking term in Eq. (57) keeping some SUSY on the lattice. However, to find such an $\mathcal{O}(a)$-improved CLR action, further detailed studies between the quantum corrections and the solutions of the CLR are necessary.

In the $\mathcal{N} = 4$ case with the CLR, the number of exact SUSY is greater than the other lattice formulation. We can expect that a lattice theory with the CLR is highly improved and behaves very similar to the continuum theory. The results shown in this paper could be useful to construct the SUSY action with a modified Leibniz rule in higher dimensions.

Acknowledgements

We would like to thank So Matsuura, Katsumasa Nakayama, and Fumihiko Sugino for their helpful comments. This work was supported by Japan Society for the Promotion of Science (JSPS) KAKENHI Grant Numbers JP16K05328, JP19K03853 and the CUniverse research promotion project of Chulalongkorn University (Grant CUAASC).

Funding

Open Access funding: SCOAP[3].

Appendix A. More about the CLR

A.1. Solutions for other difference operators

The solutions of the CLR for the forward difference operator and a symmetric difference operator $\nabla_S = \frac{1}{2}(\nabla_+ - \nabla_-)$ are presented. For any difference operator ∇, the CLR is defined in the same manner as Eq. (30). By repeating the same procedures as in Sect. 3.2, we find that Eq. (30) can be written as

$$\sum_n \nabla\phi_n W_n = 0. \tag{A.1}$$

It is then easy to find a local solution of Eq. (A.1):

$$W_n = \begin{cases} \frac{U(\phi_{n+1})-U(\phi_n)}{\phi_{n+1}-\phi_n} & \text{for } \nabla = \nabla_+ \\ \frac{U(\phi_{n+1})-U(\phi_{n-1})}{\phi_{n+1}-\phi_{n-1}} & \text{for } \nabla = \nabla_S. \end{cases} \tag{A.2}$$

The same discussions as mentioned in Sect. 3.2 tell us that the solutions in Eq. (A.2) are well-defined local functions that reproduce $W(\phi_n)$ up to $\mathcal{O}(a)$.

A.2. The m-body CLR

We now consider a case of $W(\phi) = \sum_{m=0}^{\infty} c_m \phi^m$ with coupling constants c_m. Then the lattice superpotential W_n is also expressed as an expansion:

$$W_n \equiv \sum_{\ell=0}^{\infty} c_\ell [\phi]_n^\ell \tag{A.3}$$

with[4]

$$[\phi]_n^\ell \equiv \sum_{m_1,m_2,\ldots,m_\ell} M_{n,m_1,m_2,\ldots,m_\ell}\phi_{m_1}\phi_{m_2}\cdots\phi_{m_\ell}. \tag{A.4}$$

Here we assume that $M_{n,m_1,m_2,\ldots,m_\ell}$ is totally symmetric for $m_1, m_2, \ldots, m_\ell$ except for the first index n and $[1]_n^\ell = 1$ as an overall normalization. The locality condition is strictly defined as

$$|M_{n,m_1,m_2,\ldots,m_\ell}| < C\exp\{-\rho|n-m_k|\} \quad \text{for all } k = 1,\ldots,\ell \tag{A.5}$$

where C and $\rho > 0$ are some positive constants. The summation in Eq. (A.4) is well defined because it is absolutely convergent for Eq. (A.5).

The CLR in Eq. (17) is shown to be

$$\sum_n \Big\{\nabla_{nm_0}M_{n,m_1,m_2,\ldots,m_{\ell-1},m_\ell} + \nabla_{nm_1}M_{n,m_2,m_3,\ldots,m_\ell,m_0} + \cdots + \nabla_{nm_\ell}M_{n,m_0,m_1,\ldots,m_{\ell-2},m_{\ell-1}}\Big\} = 0, \tag{A.6}$$

which is referred to as the m-body CLR. It is easy to show that Eq. (A.6) is equivalent to Eq. (17). We should note that the indices $m_0, m_1, m_2, \ldots, m_\ell$ cyclically appear in Eq. (A.6). This is the reason why we called Eq. (17) the *cyclic* Leibniz rule.

The solutions of the m-body CLR for the backward difference operator can be read from Eq. (18) using

$$M_{n,m_1,m_2,\ldots,m_\ell} = \frac{1}{\ell!}\frac{\partial^\ell W_n}{\partial\phi_{m_1}\partial\phi_{m_2}\cdots\partial\phi_{m_\ell}}\bigg|_{c_m=1,\phi=0}. \tag{A.7}$$

We have

$$M_{n,m} = \frac{1}{2}\left(\delta_{nm} + \delta_{n-1,m}\right), \tag{A.8}$$

$$M_{n,m,k} = \frac{1}{6}\left(2\delta_{nm}\delta_{nk} + \delta_{n-1,m}\delta_{nk} + \delta_{nm}\delta_{n-1,k} + 2\delta_{n-1,m}\delta_{n-1,k}\right), \tag{A.9}$$

$$\begin{aligned} M_{n,m,k,l} = \frac{1}{12}(&3\delta_{n,m}\delta_{nk}\delta_{nl} + \delta_{n-1,m}\delta_{nk}\delta_{nl} + \delta_{nm}\delta_{n,k+1}\delta_{nl} + \delta_{nm}\delta_{nk}\delta_{n-1,l} \\ &+ \delta_{n-1,m}\delta_{n-1,k}\delta_{nl} + \delta_{n-1,m}\delta_{nk}\delta_{n-1,l} + \delta_{nm}\delta_{n-1,k}\delta_{n-1,l} + 3\delta_{n-1,m}\delta_{n-1,k}\delta_{n-1,l}), \end{aligned} \tag{A.10}$$

and so on.

The explicit forms of a solution $M_{n,m_1,m_2,\ldots,m_\ell}$ for the forward difference operator are obtained by replacing the lattice site $n-1$ by $n+1$ in Eqs. (A.8), (A.9), and (A.10). Those for the symmetric difference operator $\nabla_S = \frac{1}{2}(\nabla_+ + \nabla_-)$ are also obtained by similar replacement of the lattice site.

[4] The simplest example of M (but it is not a solution of the CLR) is $M_{n,m_1,m_2,\ldots,m_\ell} = \delta_{nm_1}\delta_{nm_2}\cdots\delta_{nm_\ell}$. Then the lattice action (16) coincides with the naive one owing to $W_n = W(\phi_n)$ and $W'_{nm} = W'(\phi_n)\delta_{nm}$. We can express a scattering of lattice variables around the site n by $M_{n,m_1,m_2,\ldots,m_\ell}$.

Appendix B. Weak coupling expansion

The weak coupling expansion of the first excited energy is presented at one-loop order for the naive, CG, and CLR actions. We perform the lattice perturbation theory on the infinite volume lattice. The first excited energies are evaluated as effective masses obtained from the two-point correlation functions. In this section, we assume that $m > 0$ and take $a = 1$ for simplicity.

B.1. Perturbative calculation on the infinite volume lattice

The free part of a lattice action S can be expressed in the momentum space as

$$S_{\text{free}} = \int_{-\pi}^{\pi} \frac{dp}{2\pi} \left\{ \frac{1}{2} D_0^{-1}(p)\phi(-p)\phi(p) + S_0^{-1}(p)\bar{\psi}(-p)\psi(p) \right\}, \tag{B.1}$$

where $D_0(p)$ and $S_0(p)$ are bare propagators of the boson and the fermion, respectively. The concrete form of $D_0(p)$ and $S_0(p)$, which depends on S_{free}, are obtained by the Fourier transformation for a lattice variable φ_n:

$$\varphi(p) = \sum_{n\in\mathbb{Z}} \mathrm{e}^{ipn}\varphi_n, \tag{B.2}$$

$$\varphi_n = \int_{-\pi}^{\pi} \frac{dp}{2\pi} \mathrm{e}^{-ipn}\varphi(p) \tag{B.3}$$

with useful identities $\delta_{n0} = \int_{-\pi}^{\pi} \frac{dp}{2\pi} \mathrm{e}^{ipn}$ $(n \in \mathbb{Z})$ and $\varphi(p + 2\pi n) = \varphi(p)$ for $n \in \mathbb{Z}$.

The two-point correlation functions are defined as

$$D_{nl} \equiv \langle \phi_n \phi_l \rangle = \int_{-\pi}^{\pi} \frac{dp}{2\pi} D(p) e^{-ip(n-l)}, \tag{B.4}$$

$$S_{nl} \equiv \langle \psi_n \bar{\psi}_l \rangle = \int_{-\pi}^{\pi} \frac{dp}{2\pi} S(p) e^{-ip(n-l)}, \tag{B.5}$$

where $D(p)$ and $S(p)$ are the full propagators. We have $D_{nl} = D_{n-l,0}$ and $S_{nl} = S_{n-l,0}$ as a result of the translational invariance. The free two-point correlation functions $(D_0)_{nl}$ and $(S_0)_{nl}$ are calculated from Eqs. (B.4) and (B.5) with $D_0(p)$ and $S_0(p)$ using the complex integral with $z = e^{ip}$.

The full propagators can be evaluated in the weak coupling expansion from D_0, S_0, and the boson and fermion self-energies Π_{nl} and Σ_{nl}. As is well known, D_{nl} is given by an infinite series:

$$D_{nl} = (D_0)_{nl} - (D_0 \Pi D_0)_{nl} + (D_0 \Pi D_0 \Pi D_0)_{nl} - \cdots . \tag{B.6}$$

Thus we have

$$D_{nl} = \left(\frac{1}{D_0^{-1} + \Pi} \right)_{nl}. \tag{B.7}$$

Similarly,

$$S_{nl} = \left(\frac{1}{S_0^{-1} + \Sigma} \right)_{nl}. \tag{B.8}$$

Once Π_{nl} and Σ_{nl} are evaluated at the n-loop level, D_{nl} and S_{nl} are obtained at the same order.

The effective masses $m^B_{\rm eff}$ and $m^F_{\rm eff}$ are read from the large distance behavior of D_{nl} and S_{nl}. For $|n-l| \gg 1$,

$$D_{nl} \approx Ce^{-m^B_{\rm eff}|n-l|}, \tag{B.9}$$

$$S_{nl} \approx C'\theta_{n,l}e^{-m^F_{\rm eff}|n-l|} \tag{B.10}$$

with

$$\theta_{n,l} \equiv \begin{cases} 1 & \text{for } n \geq l \\ 0 & \text{for } n < l. \end{cases} \tag{B.11}$$

At the one-loop level, the self-energies provide the shifts of masses Δm in $D_0^{-1}(p)$ and $S_0^{-1}(p)$ via Eqs. (B.7) and (B.8). The one-loop effective masses $m^{B,F}_{\rm eff}$ are actually obtained from the formulas of tree-level effective masses $m^{B,F}_{0,\rm eff}$ with $m \to m + \Delta m$.

B.2. The naive action

We begin with the case of the naive action (12) whose $D_0(p)$ and $S_0(p)$ are given by

$$D_0(p) \equiv \frac{1}{2(1-\cos p)+m^2}, \tag{B.12}$$

$$S_0(p) \equiv \frac{1}{1-e^{ip}+m}. \tag{B.13}$$

The free boson propagator in the position space is evaluated from Eq. (B.4):

$$(D_0)_{nl} = -\frac{1}{2\pi i}\oint dz \frac{z^{-n+l}}{z^2-(m^2+2)z+1}, \tag{B.14}$$

where the contour is a unit circle with the center at the origin with $z = e^{ip}$. It is easily shown that

$$(D_0)_{nl} = \frac{e^{-m^B_{0,\rm eff}|n-l|}}{\sqrt{m^4+4m^2}}, \tag{B.15}$$

where

$$m^B_{0,\rm eff} = -\log\left(1+\frac{m^2}{2}-\frac{1}{2}\sqrt{m^4+4m^2}\right). \tag{B.16}$$

Similarly,

$$(S_0)_{nl} = \theta_{n,l}\frac{e^{-m^F_{0,\rm eff}|n-l|}}{1+m}, \tag{B.17}$$

where

$$m^F_{0,\rm eff} = \log(1+m), \tag{B.18}$$

and $\theta_{k,l}$ is given by Eq. (B.11). Note that $m^B_{0,\rm eff}$ and $m^F_{0,\rm eff}$ are positive for $m > 0$ and coincide for $m \ll 1$.

At the one-loop level, the boson and fermion self-energies are obtained as

$$\Pi(p) = 6\lambda m^2\left(\frac{2}{\sqrt{4+m^2}} - \frac{1}{1+m}\right), \tag{B.19}$$

$$\Sigma(p) = \frac{3\lambda m}{\sqrt{4+m^2}}. \tag{B.20}$$

The one-loop self-energies provide different corrections to the mass $m \to m + \Delta m_{B,F}$ where Δm_B and Δm_F are identified from Eqs. (B.19) and (B.20), respectively.

The one-loop effective masses are obtained by inserting $m + \Delta m_{B,F}$ into Eqs. (B.16) and (B.18):

$$\frac{E_1^B}{m} = 1 + 3m\lambda - \frac{1}{24}m^2 - \frac{27}{8}m^2\lambda + O(\lambda^2, m^3), \tag{B.21}$$

$$\frac{E_1^F}{m} = 1 + \frac{3}{2}\lambda - \frac{1}{2}m - \frac{3}{2}m\lambda + \frac{1}{3}m^2 + \frac{21}{16}m^2\lambda + O(\lambda^2, m^3). \tag{B.22}$$

We should note that E_1^B is different from E_1^F even in the continuum limit $ma \to 0$ as a result of the one-loop effect.

B.3. The CG action

The free propagators of the CG action (13) are

$$D_0(p) = \frac{1}{2(1-\cos p) + m^2 + 2m(1-\cos p)}, \tag{B.23}$$

$$S_0(p) = \frac{1}{1 - e^{ip} + m}. \tag{B.24}$$

Note that the fermion propagator is the same as that of the naive action. A similar calculation to that done around Eq. (B.14) tells us that the effective masses at the tree level are degenerated as

$$m^B_{0,\mathrm{eff}} = m^F_{0,\mathrm{eff}} = \log(1+m), \tag{B.25}$$

which is positive for $m > 0$.

The self-energies are calculated at the one-loop level as

$$\Pi(p) = \Delta m[2m + 2(1-\cos p)], \tag{B.26}$$

$$\Sigma(p) = \Delta m, \tag{B.27}$$

where

$$\Delta m \equiv \frac{3\lambda m}{2+m}. \tag{B.28}$$

These give the same correction to the boson mass and the fermion mass up to $O(\lambda)$. The one-loop effective masses are evaluated from Eq. (B.25) with $m + \Delta m$. We thus obtain that

$$\frac{E_1}{m} = 1 + \frac{3}{2}\lambda - \frac{1}{2}m - \frac{9}{4}m\lambda + \frac{1}{3}m^2 + \frac{21}{8}m^2\lambda + O(\lambda^2, m^3), \tag{B.29}$$

for $E_1 \equiv m^B_{\mathrm{eff}} = m^F_{\mathrm{eff}}$ owing to an exact SUSY.

B.4. The CLR action

The free propagators of the CLR action (35) are given by

$$D_0(p) \equiv \frac{1}{2(1-\cos p) + m^2(1+\cos p)/2}, \tag{B.30}$$

$$S_0(p) \equiv \frac{1}{1 - e^{ip} + m(1 + e^{ip})/2}. \tag{B.31}$$

The tree-level effective masses are degenerated as

$$m^B_{0,\mathrm{eff}} = m^F_{0,\mathrm{eff}} = \log\left(\frac{1 + \frac{m}{2}}{1 - \frac{m}{2}}\right), \tag{B.32}$$

which is positive for $m > 0$.

The one-loop self-energies are given by

$$\Pi(p) = m\Delta m(1 + \cos p), \tag{B.33}$$

$$\Sigma(p) = \Delta m\left(\frac{1 + e^{ip}}{2}\right), \tag{B.34}$$

where

$$\Delta m = \frac{\lambda m(m + 6)}{2(m + 2)}. \tag{B.35}$$

The one-loop effective masses are read from Eq. (B.32) with $m + \Delta m$. The first excited energies for the bosonic and fermionic states are thus obtained as $E_1 \equiv m^B_{\mathrm{eff}} = m^F_{\mathrm{eff}}$:

$$\frac{E_1}{m} = 1 + \frac{3}{2}\lambda - \frac{1}{2}m\lambda + \frac{1}{12}m^2 + \frac{5}{8}m^2\lambda + O(\lambda^2, m^3), \tag{B.36}$$

owing to an exact SUSY.

The results above are obtained for the backward difference operator ∇_- and Eq. (18) for a solution of W_n. The CLR action with the forward difference operator ∇_+ and Eq. (A.2) for W_n gives the same effective masses (B.32) and (B.36).

References

[1] P. H. Dondi and H. Nicolai, Nuovo Cimento A **41**, 1 (1977).
[2] M. Kato, M. Sakamoto, and H. So, J. High Energy Phys. **0805**, 057 (2008).
[3] M. Kato, M. Sakamoto, and H. So, PoS **LATTICE2012**, 231 (2012).
[4] D. Kadoh and H. Suzuki, Phys. Lett. B **684**, 167 (2010).
[5] G. Bergner, J. High Energy Phys. **1001**, 024 (2010).
[6] K. Asaka, A. D'Adda, N. Kawamoto, and Y. Kondo, Int. J. Mod. Phys. A **31**, 1650125 (2016).
[7] N. Sakai and M. Sakamoto, Nucl. Phys. B **229**, 173 (1983).
[8] S. Catterall and E. Gregory, Phys. Lett. B **487**, 349 (2000).
[9] S. Catterall and S. Karamov, Nucl. Phys. Proc. Suppl. **106–107**, 935 (2002).
[10] Y. Kikukawa and Y. Nakayama, Phys. Rev. D **66**, 094508 (2002).
[11] A. G. Cohen, D. B. Kaplan, E. Katz, and M. Ünsal, J. High Energy Phys. **0308**, 024 (2003).
[12] A. G. Cohen, D. B. Kaplan, M. Ünsal, and E. Katz, J. High Energy Phys. **0312**, 031 (2003).
[13] F. Sugino, J. High Energy Phys. **0401**, 015 (2004).
[14] F. Sugino, J. High Energy Phys. **0403**, 067 (2004).
[15] A. D'Adda, I. Kanamori, N. Kawamoto, and K. Nagata, Nucl. Phys. B **707**, 100 (2005).
[16] F. Sugino, J. High Energy Phys. **0501**, 016 (2005).
[17] G. Bergner, T. Kaestner, S. Uhlmann, and A. Wipf, Ann. Phys. **323**, 946 (2008).
[18] D. Kadoh and H. Suzuki, Phys. Lett. B **696**, 163 (2011).
[19] D. Kadoh, PoS **LATTICE2015**, 017 (2016).
[20] D. Schaich, 36th Int. Symp. Lattice Field Theory (Lattice 2018) (2018), arXiv:1810.09282 [hep-lat] [Search INSPIRE].
[21] M. Kato, M. Sakamoto, and H. So, J. High Energy Phys. **1305**, 089 (2013).

[22] E. Witten, Nucl. Phys. B **188**, 513 (1981).
[23] E. Witten, Nucl. Phys. B **202**, 253 (1982).
[24] D. Kadoh and N. Ukita, Prog. Theor. Exp. Phys. **2015**, 103B04 (2015).
[25] M. Kato, M. Sakamoto, and H. So, Prog. Theor. Exp. Phys. **2017**, 043B09 (2017).
[26] M. Kato, M. Sakamoto, and H. So, Prog. Theor. Exp. Phys. **2018**, 121B01 (2018).
[27] J. Giedt, E. Poppitz, R. Koniuk, and T. Yavin, J. High Energy Phys. **0412**, 033 (2004).
[28] I. Kanamori, H. Suzuki, and F. Sugino, Phys. Rev. D **77**, 091502(R) (2008).
[29] C. Wozar and A. Wipf, Ann. Phys. **327**, 774 (2012).
[30] D. Kadoh and K. Nakayama, Nucl. Phys. B **932**, 278 (2018).
[31] D. Kadoh and K. Nakayama, arXiv:1812.10642 [hep-lat] [Search INSPIRE].
[32] D. Baumgartner and U. Wenger, Nucl. Phys. B **894**, 223 (2015).
[33] D. Baumgartner and U. Wenger, Nucl. Phys. B **897**, 39 (2015).
[34] D. Baumgartner and U. Wenger, Nucl. Phys. B **899**, 375 (2015).
[35] D. Kadoh, Y. Kuramashi, Y. Nakamura, R. Sakai, S. Takeda, and Y. Yoshimura, J. High Energy Phys. **1803**, 141 (2018).
[36] D. Kadoh, Y. Kuramashi, Y. Nakamura, R. Sakai, S. Takeda, and Y. Yoshimura, arXiv:1811.12376 [hep-lat] [Search INSPIRE].
[37] F. Cooper, A. Khare, and U. Sukhatme, Phys. Rept. **251**, 267 (1995).